Efficient evaluation of electron correlation along the bond-dissociation coordinate in the ground and excited ionic states with dynamic correlation suppression and enhancement functions of the on-top pair density

Oleg V. Gritsenko,[1,2] Robert van Meer,[2] and Katarzyna Pernal[1]

[1]*Institute of Physics, Lodz University of Technology, PL-90-924 Lodz, Poland*
[2]*Division of Theoretical Chemistry, VU University, NL-1081 HV Amsterdam, The Netherlands*

Calculation of the electron correlation energy E_c of ground and excited states through the partitioning and evaluation of the dynamic E_c^d and nondynamic E_c^{nd} components requires one to account for the interplay of these correlation modes as well as for the excitation effect. In this paper it is demonstrated that both local suppression of dynamic correlation (SDC) by nondynamic correlation and enhancement of dynamic correlation (EDC) due to excitation to a state of the ionic nature can be quantified with the ratio $x(\boldsymbol{r})$ between the correlated and uncorrelated on-top pair densities $\Pi(\boldsymbol{r})$. A CASΠDFT scheme is proposed, in which E_c^{nd} is calculated with the complete active space approach in a small basis, while E_c^d is calculated in the same basis with a functional of density functional theory corrected for SDC and EDC with an original correction function of $x(\boldsymbol{r})$. Correlation energies calculated with CASΠDFT along the bond-dissociation coordinate for the paradigmatic H_2 and N_2 molecules as well as for the C_2 molecule with strong nondynamic correlation at the equilibrium agree well with the reference data, thus providing a proof of concept for CASΠDFT.

I. INTRODUCTION

Though somewhat arbitrary, the partitioning of the Coulomb electron correlation to dynamic and nondynamic (static) modes is useful for its efficient calculation and meaningful interpretation. In the latter mode correlated electrons are placed to the separated spatial regions and the paradigmatic system in this case is the dissociating H_2 molecule, in which "left-right" correlation [1] places two electrons with the opposite spins to the different H atoms. The energy of nondynamic correlation E_c^{nd} can be evaluated with the complete active space (CAS) (n, n) configuration interaction (CI) [2–4], in which $2n$ electrons are distributed in all possible ways among the bonding and antibonding orbitals associated with n valence bonds.

Dynamic correlation is characterized with a rather short-range concerted configuration of electrons arranged to reduce their mutual repulsion. Its particular modes in atoms are radial "in-out" and "angular" correlations; the latter is taken into account in *ab initio* wave function methods by the inclusion of higher angular momentum functions [5]. For atoms its energy E_c^d can be efficiently evaluated with correlation functionals [6–9] of density functional theory (DFT). In molecules dynamic correlation can be strongly influenced with other many-electron effects, such as the above mentioned nondynamic correlation.

One of the topics of this paper is the elucidation of the opposite trends, which exhibits dynamic correlation in the molecular ground state and in the excited states of ionic nature. The latter states are the most important low-lying excited states within the small CAS approach. It will be demonstrated that in the ground-state dynamic correlation experiences the suppression with nondynamic correlation, which gradually

increases with the bond stretching. In the excited state dynamic correlation exhibits the enhancement due to the ionic character of the state. The CAS on-top pair density $\Pi^{CAS}(\boldsymbol{r})$ is proposed as the descriptor of these trends. In general, $\Pi(\boldsymbol{r})$ is defined as the pair density of the wave function Ψ evaluated at the electron coalescence point $\boldsymbol{r}_1 = \boldsymbol{r}_2 = \boldsymbol{r}$,

$$\Pi(\boldsymbol{r}) = N(N-1) \int |\Psi(\boldsymbol{x}_1, \boldsymbol{x}_2, \ldots, \boldsymbol{x}_N)|^2$$
$$\times \, d\sigma_1 d\sigma_2 d\boldsymbol{x}_3 \ldots d\boldsymbol{x}_N|_{\boldsymbol{r}_1=\boldsymbol{r}_2=\boldsymbol{r}}, \quad (1)$$

where $\boldsymbol{x} \equiv \{\boldsymbol{r}, \sigma\}$ stands for both spatial $\boldsymbol{r}$ and spin σ coordinates [10].

Another topic of this paper is the efficient evaluation of the total correlation energy E_c,

$$E_c = E_c^{nd} + E_c^d, \quad (2)$$

with the combined approach, in which E_c^{nd} is obtained with CAS(n, n), while E_c^d is calculated with a (corrected) DFT functional. In the ground state the main problem of such an approach is to avoid the double counting of electron correlation coming from different methods [11–14]. Recently, to avoid this problem altogether, the method was proposed [15], in which the total exchange-correlation (xc) energy E_{xc} is calculated with a DFT functional. At variance with the conventional DFT, this xc functional employs $\Pi^{CAS}(\boldsymbol{r})$ as an additional argument, in order to be able to switch between dynamic and nondynamic correlation modes, when calculating $E_{xc}[\rho, \Pi^{CAS}]$. This switching is achieved by introducing an artificial electron spin polarization in the singlet state evaluated from $\Pi^{CAS}(\boldsymbol{r})$ [15]. A promising way to avoid the double-counting problem is based on the range-separation approach, which combines the

multiconfigurational self-consistent field (MCSCF) approach to treat the long-range part of the electron-electron interaction with the short-range DFT functional [16].

In this paper, we follow the earlier work [11,13], in which the $CAS(n,n)$ contribution and the proper spin-restricted description of singlet systems are fully retained, so E_c^{nd} is calculated as the difference,

$$E_c^{nd} = E^{CAS} - E^{HF}, \quad (3)$$

between the CAS E^{CAS} and Hartree-Fock (HF) E^{HF} to-tal electronic energies. In its turn, E_c^d is calculated as follows:

$$E_c^d = \int P[\Pi^{CAS}](\boldsymbol{r})\epsilon_c^{DFT}[\rho](\boldsymbol{r})d\boldsymbol{r}, \quad (4)$$

where $\epsilon_c^{DFT}[\rho](\boldsymbol{r})$ is the energy density of a suitable conventional DFT correlation functional, in this paper $\epsilon_c^{LYP}[\rho](\boldsymbol{r})$ of the popular Lee-Yang-Parr (LYP) correlation functional [7,17] is employed. Previously, the LYP functional was employed in the combined CAS and DFT approach in Ref. [13], though in a different from (4) way, in which Π^{CAS} was directly inserted into the LYP expression for ϵ_c^{DFT}. In this paper, the DFT energy density is corrected in (4) with the multiplicative correction function $P[\Pi^{CAS}]$, a functional of Π^{CAS} and ρ (see below the form of this functional).

The CASΠDFT approach [Eqs. (3) and (4)] allows one to carry out the calculations of E_c of (2) in a small basis. Indeed, the main purpose of using large basis sets in the conventional CI approach is a reliable evaluation of dynamic correlation. However, DFT calculations are, usually, not so sensitive to the basis choice. Then, the use of a small basis leads to a tremendous speed-up of calculations. Due to this, such calculations become a rather hot topic in the literature. In particular, approximate methods, such as tight-binding DFT (DFTB) [18], adapted to the minimal basis set make possible calculations of very large supermolecular systems and molecular complexes.

In this paper, the correction function $P[\Pi^{CAS}]$ is proposed, which accounts for both the above mentioned suppression of dynamic correlation (SDC) in the ground state and the enhancement of dynamic correlation (EDC) in the excited ionic state. In Sec. II the ratio $x(\boldsymbol{r})$ of $\Pi^{CAS}(\boldsymbol{r})$ to its uncorrelated counterpart is put forward as the descriptor of the changes of the effective conditional density due to nondynamic correlation and excitation. In Sec. III the correction function $P(x(\boldsymbol{r}))$ is introduced for the whole range of the $x(\boldsymbol{r})$ variation. In Sec. IV CASΠDFT with the proposed $P(x(\boldsymbol{r}))$ is applied to calculation of E_c along R for the ground $^1\Sigma_g^+$ states of the paradigmatic molecules H_2 and N_2. In Sec. V E_c is evaluated for the C_2 molecule, in which rather strong nondynamic correlation takes place already at the equilibrium R. In Sec. VI CASΠDFT is applied to calculation of E_c^d along R for the excited ionic $^1\Sigma_u^+$ state of the H_2 molecule. The results of the calculations in small basis sets agree well with the reference data. In Sec. VII the conclusions are drawn.

II. ON-TOP PAIR DENSITY RATIO AS A LOCAL DESCRIPTOR OF NONDYNAMIC CORRELATION AND EXCITATION EFFECTS

As was already mentioned in the introduction, the $CAS(n,n)$ wave function provides the basic effect of non-dynamic correlation in the ground state. For example, in the paradigmatic case of the H_2 molecule the CAS(1,1) ground state Ψ_g^{CAS} is the linear combination,

$$\Psi_g^{CAS} = c_1\Psi_0 - c_2\Psi_{gg}^{uu} = (c_1 - c_2)\Psi_0 + \sqrt{2}c_2\Psi^{HL}, \quad (5)$$

of the Hartree-Fock (HF) reference Ψ_0 and its double excitation Ψ_{gg}^{uu}. The former represents the $1\sigma_g^2$ configuration, while the latter is the $1\sigma_u^2$, where $1\sigma_g$ and $1\sigma_u$ are the bonding occupied and antibonding virtual molecular orbitals (MOs) of H_2.

Equivalently, Ψ_g^{CAS} is written in (5) as the linear combination of Ψ_0 and the Heitler-London (HL)-type wave function Ψ^{HL}, the latter includes the $1\sigma_g^2$ and $1\sigma_u^2$ configurations with the equal weights. It is Ψ^{HL}, which introduces nondynamic correlation in Ψ_g^{CAS}. On the other hand, the CAS(1,1) excited state Ψ_u^{CAS} of the $^1\Sigma_u^+$ symmetry is the correlationless excited HF state $\Psi_u^{CAS} \equiv \Psi_g^u$, which represents the spin-adapted $1\sigma_g 1\sigma_u$ configuration.

The local effect of nondynamic correlation in the ground state and the effect of excitation on the electron distribution can be quantified by the comparison of the CAS on-top pair density $\Pi^{CAS}(\boldsymbol{r})$ with its uncorrelated counterpart, the Hartree product $\Pi^H(\boldsymbol{r})$ of the electron densities ρ,

$$\Pi^H(\boldsymbol{r}) = \rho(\boldsymbol{r}_1)\rho(\boldsymbol{r}_2)|_{\boldsymbol{r}_1=\boldsymbol{r}_2=\boldsymbol{r}} = \rho^2(\boldsymbol{r}). \quad (6)$$

Valuable information is produced with the (doubled) ratio of these quantities,

$$x(\boldsymbol{r}) = \frac{2\Pi^{CAS}(\boldsymbol{r})}{\Pi^H(\boldsymbol{r})} = \frac{2\Pi^{CAS}(\boldsymbol{r})}{\rho^2(\boldsymbol{r})} = \frac{2\rho_{cond}^{(\uparrow\downarrow)CAS}(\boldsymbol{r}|\boldsymbol{r})}{\rho(\boldsymbol{r})}, \quad (7)$$

which is, simultaneously, the ratio of the opposite-spin component $\rho_{cond}^{(\uparrow\downarrow)CAS}(\boldsymbol{r}|\boldsymbol{r})$ of the CAS on-top conditional density to its uncorrelated counterpart $\frac{1}{2}\rho(\boldsymbol{r})$. In general, the conditional density $\rho_{cond}(\boldsymbol{r}_2|\boldsymbol{r}_1)$ is defined as the ratio of the pair density $\Pi(\boldsymbol{r}_1, \boldsymbol{r}_2)$ to the electron density $\rho(\boldsymbol{r}_1)$,

$$\rho_{cond}(\boldsymbol{r}_2|\boldsymbol{r}_1) = \frac{\Pi(\boldsymbol{r}_1, \boldsymbol{r}_2)}{\rho(\boldsymbol{r}_1)}, \quad (8)$$

and it gives the density of the remaining electrons at $\boldsymbol{r}_2$ when the reference electron is at $\boldsymbol{r}_1$. Then, the stronger the nondynamic correlation is, the harder it pushes other electrons of the opposite spin from the vicinity of the reference electron of a given spin, which makes $\Pi^{CAS}(\boldsymbol{r})$, $\rho_{cond}^{(\uparrow\downarrow)CAS}(\boldsymbol{r}|\boldsymbol{r})$, and the ratio (7) smaller.

Figures 1–3 display the ratio (7) calculated for the ground state of the H_2 and N_2 molecules as a function $x(z)$ of the bond axis coordinate z. For H_2 the calculations are performed in the double-zeta (DZ) basis of Dunning [19] with only two basis functions per atom. For N_2 the cc-pVDZ basis [20] is used without the d functions, i.e., with only nine basis functions per atom. The CAS CI calculations are carried out, with the $CAS(n,n)$ configurations being augmented with single excitations from the active to the outer space. This
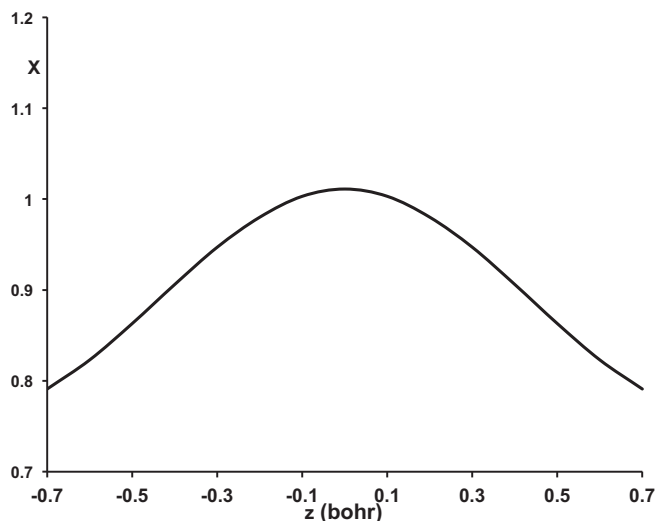
FIG. 1. The ratio x of the CAS on-top pair density to its un-correlated counterpart along the bond axis z of the ground-state H_2 molecule at R(H-H)=1.4 bohr. The H nuclei are placed at -0.7 and 0.7 bohr.

FIG. 3. The ratio x of the CAS on-top pair density to its un-correlated counterpart along the bond axis z of the ground-state N_2 molecule at R(N-N)=3 $\mathring{A}$ = 5.67 bohr. The N nuclei are placed at -2.835 and 2.835 bohr.

inclusion improves the resultant electron density in the sense that the occupations of all its natural orbitals (NOs) become larger than 10^{-7}, which is the required threshold in the employed GAMESS-US package [21,22]. This does not appreciably change the major occupations of the lowest NOs and $x(z)$ calculated for the ground-state H_2 displays the same trend as that obtained previously in Ref. [23] with the CAS SCF.

Figure 1 describes the effect of nondynamic correlation in the ground state of H_2 with the decrease of $x(z)$ up to 0.8, when approaching the nuclei. Due to the dominating contribution of the HL-type wave function in (5), this effect is much stronger for the stretched H_2 (see Fig. 2). Indeed, strong nondynamic correlation causes vanishing of $x(z)$ in the
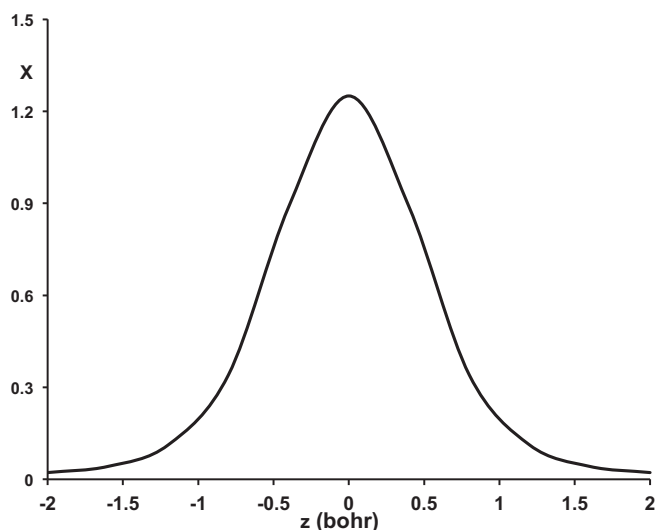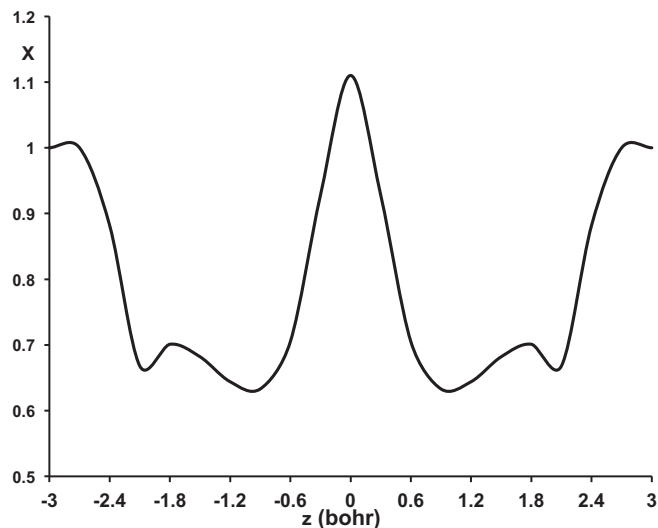

FIG. 2. The ratio x of the CAS on-top pair density to its un-correlated counterpart along the bond axis z of the ground-state H_2 molecule at R(H-H)=4 bohr. The H nuclei are placed at -2 and 2 bohr.

regions of the H atoms. On the other hand, the bond midpoint region is distinguished with relatively high $x(z)$ values (see Figs. 1 and 2). Apparently, it is the dynamic correlation, which is responsible for correlating electrons in this region.

For the N_2 molecule $x(z)$ exhibits the same qualitative trends as for H_2. One can see from Fig. 3 that $x(z)$ distinguishes between the outer valence and inner regions. In the former, the strong nondynamic correlation from the CAS(3,3) wave function lowers $x(z)$ to ca. 0.65. The apparent inability of CAS(3,3) to efficiently correlate electrons in the inner regions keeps $x(z)$ close to 1 in these regions.

Remarkably, excitation to the ionic state produces the opposite effect on $x(z)$ compared to that of nondynamic correlation (see Figs. 4 and 5). Indeed, $x(z)$ calculated for the $1^1\Sigma_u^+$ state of H_2 at $R = 2$ bohr is substantially larger than 1, reaching the value of ca. 1.6 at the nuclei (see Fig. 4). In the bond midpoint region $x(z)$ vanishes due to the node of the excited wave function. For the larger $R = 4$ bohr $x(z)$ further increases in the atomic regions, approaching the value $x(z) = 2$ (see Fig. 5).

For the considered excited state the values $x(z) > 1$ are physically meaningful; they reflect its ionic nature. Indeed, in an ionic state excitation squeezes two electrons of the opposite spins in the same atomic region. As a result, in the vicinity of the reference electron with the spin α we have a single electron with the spin β, so in the ideal ionic situation the on-top pair density tends to $\rho(\boldsymbol{r})\rho(\boldsymbol{r})$, which is twice as large as the corresponding Hartree product in the denominator of (7). From this rationalization it follows that the increase of $x(z)$ in the atomic regions, when going from $R = 2$ to $R = 4$ bohr implies the increase of the ionic character of the $1^1\Sigma_u^+$ state with the molecular stretching.

Now, we turn to the opposite trends in dynamic correlation caused by nondynamic correlation and excitation to the ionic state. One can introduce a physical notion of the suppression of dynamic correlation (SDC) with nondynamic correlation.
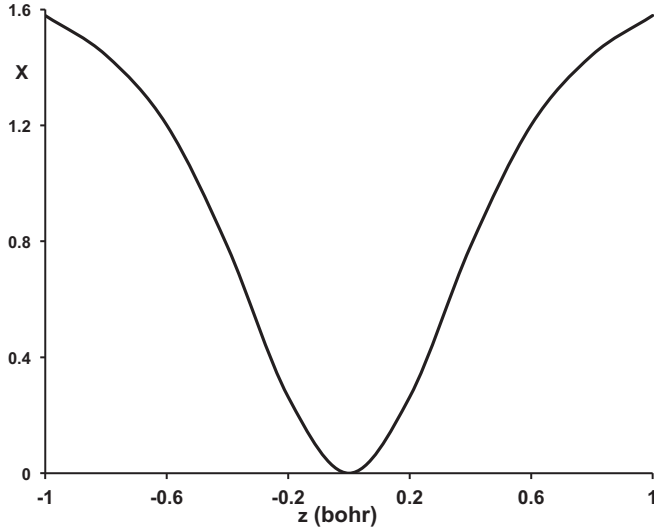
FIG. 4. The ratio x of the CAS on-top pair density to its uncorrelated counterpart along the bond axis z of the excited-state H_2 molecule at R(H-H)=2 bohr. The H nuclei are placed at -1 and 1 bohr.

SDC means that, placing electrons to the separated spatial regions, nondynamic correlation makes irrelevant their shorter-range dynamic correlation. Locally, SDC can be viewed as follows. Nondynamic correlation reduces the repulsion of the reference electron at r_1 due to the reduction of the conditional density $\rho_{\text{cond}}^{(\uparrow\downarrow)\text{CAS}}(r_2|r_1)$ of other electrons with the opposite spin in its vicinity. Naturally, this weakens further reduction of the repulsion due to dynamic correlation of the electrons. Then, as follows from the relation (7), the regions with SDC are characterized with the reduced $x(r) < 1$. These regions are displayed in Figs. 1–3.
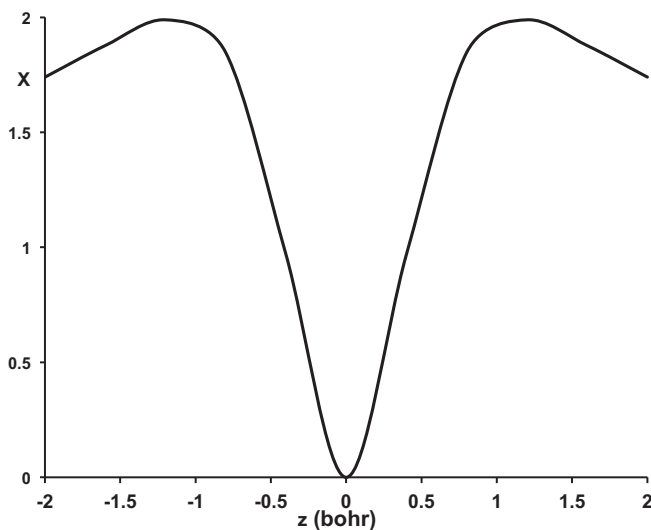

FIG. 5. The ratio x of the CAS on-top pair density to its uncorrelated counterpart along the bond axis z of the excited-state H_2 molecule at R(H-H)=4 bohr. The H nuclei are placed at -2 and 2 bohr.

On the other hand, squeezing of electrons upon excitation to an ionic state increases the repulsion of the reference electron at r_1 due to the increase of the conditional density $\rho_{\text{cond}}^{(\uparrow\downarrow)\text{CAS}}(r_2|r_1)$. Naturally, this increase can be partially compensated with the enhanced dynamic correlation (EDC) of the electrons. Then, as follows from the relation (7), the regions with EDC are characterized with the enhanced $x(r) > 1$. These regions are displayed in Figs. 4 and 5.

III. CASΠDFT CORRECTION FUNCTION FOR THE WHOLE RANGE OF THE $x(r)$ VARIATION

The description of local effects of nondynamic correlation and excitation in terms of the "effective" conditional density and the related argument $x(r)$ naturally serves for designing of the correction function in the CASΠDFT expression (4) for E_c^d. Indeed, the above mentioned reduction of $\rho_{\text{cond}}^{(\uparrow\downarrow)\text{CAS}}$ due to nondynamic correlation effectively moves the correlation energy density in (4) to lower density. This can be represented with the SDC segment $P^{\text{SDC}}[x]$ of the correction function, $P[\Pi^{\text{CAS}}] \equiv P^{\text{SDC}}[x] \leqslant 1$ for $x(r) \leqslant 1$. The increase of $\rho_{\text{cond}}^{(\uparrow\downarrow)\text{CAS}}$ due to excitation to the ionic state effectively moves the correlation energy density to higher density. This can be represented with the EDC segment $P^{\text{EDC}}[x]$ of the correction function, $P^{\text{SDC}}[x] > 1$ for $x(r) > 1$.

These two segments constitute the total correction function $P[x]$ of this paper defined for the whole range of the $x(r)$ variation,

$$P[x] = \begin{cases} P^{\text{SDC}}(x(r)) \leqslant 1, & x \leqslant 1 \\ P^{\text{EDC}}(x(r)) > 1, & x > 1 \end{cases}. \quad (9)$$

Here, $P^{\text{SDC}}(x(r))$ is the following [1/1] Padé approximant $P_{[1/1]}^{\text{SDC}}(x(r))$,

$$P_{[1/1]}^{\text{SDC}}(x(r)) = \frac{ax(r)}{1 + bx(r)}. \quad (10)$$

The form of $P_{[1/1]}^{\text{SDC}}(x(r))$ is chosen to provide the correct SDC asymptotics in the $x \to 0$ and $x \to 1$ limits. In particular, $P_{[1/1]}^{\text{SDC}}(x(r) \to 0)$ vanishes reflecting strong SDC with strong nondynamic correlation in this limit. This leads to the vanishing at r correlation energy density, the integrand in (4).

The opposite limit $x \to 1$ represents a weak nondynamic correlation, which does not suppress dynamic correlation, so $P_{[1/1]}^{\text{SDC}}(1) = 1$. This condition fixes one of two parameters a and b of the [1/1] Padé approximant, $b = a - 1$. The single free parameter a of (10) is fitted to reproduce the reference data for the ground state of H_2 (see Sec. IV).

In its turn, $P^{\text{EDC}}(x(r))$ of the following form,

$$P^{\text{EDC}}(x(r)) = c\sqrt[4]{x(r)} - d(x(r) - g)^2, \quad (11)$$

is used in (9). The condition $P^{\text{EDC}}(1) = 1$ of the continuity of the total function (9) fixes one of the three parameters of (11),

$$d = \frac{c - 1}{(1 - g)^2}. \quad (12)$$

The parameters c and g of (11) are fitted to reproduce the reference data for the excited $^1\Sigma_u^+$ state of H_2. Their actual values as well as the justification of the two-term form of (11) will be given in Sec. VI.
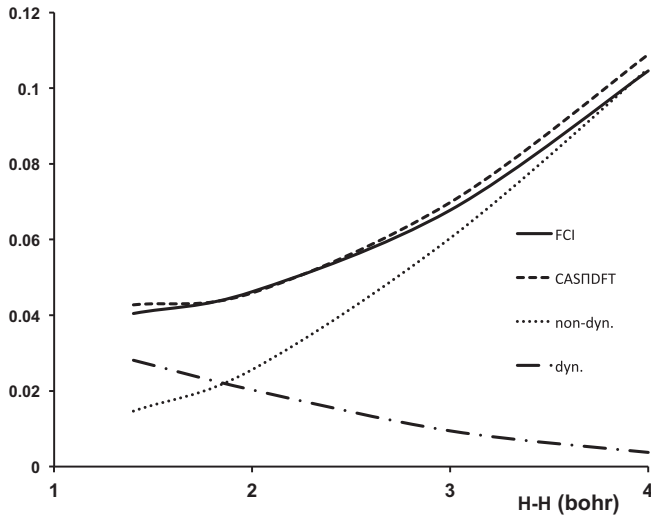
FIG. 6. The (minus) full CI correlation energy (FCI), the total CAS and corrected DFT correlation energy (CASΠDFT), and the nondynamic (non-dyn) and dynamic (dyn) contributions (in hartree) to the latter calculated along the dissociation coordinate of the H_2 molecule.

Equations (2)–(4) and (9)–(12) represent the CASΠDFT approach of this paper. We would like to emphasize that in the subsequent ground- and excited-state calculations in Secs. IV–VI the total two-segment function (9) and not its individual segments (10) and (11) will be used in all cases.

IV. GROUND-STATE CORRELATION ENERGY ALONG THE BOND-DISSOCIATION COORDINATE WITH CASΠDFT

Figure 6 and Tables I–III present the results of the CASΠDFT ground-state calculations of the correlation energy for the paradigmatic H_2 and N_2 molecules along the bond-dissociation coordinate as well as for the C_2 molecule at the equilibrium. The calculations are performed with the same wave functions and densities obtained in the same small basis sets as those employed for the calculation of $x(r)$ of the previous section. The parameter $a = 0.35$ is chosen in the SDC segment (10) of the correction function (9).

Figure 6 displays the ground-state correlation energy E_c together with its dynamic E_c^d and nondynamic E_c^{nd} components calculated with the present CASΠDFT with CAS(1,1) along the bond-dissociation coordinate $R(H-H)$ of the paradig-

matic H_2 molecule. The CASΠDFT E_c is compared with the reference full CI (FCI) one calculated in the large augmented correlation-consistent quadruple-zeta (aug-cc-pVQZ) basis [20].

One can see from Fig. 6 that the CASΠDFT E_c closely reproduces the reference FCI one at all distances considered with, basically, the chemical accuracy of 0.001–0.002 hartree. The absolute E_c value steadily increases with R, due to the gradual development of strong nondynamic correlation. The interplay between dynamic and nondynamic correlation components is vividly depicted with crossing of the E_c^d and E_c^{nd} curves.

As one can expect, at the equilibrium distance $R = 1.4$ bohr dynamic correlation prevails. However, after the curve crossing point at R ca. 1.8 bohr nondynamic correlation dominates. The SDC effect becomes very visible after $R = 2.5$ bohr and at larger R E_c^d vanishes. From this and the comparison with the reference FCI curve one can conclude, that the SDC effect is well represented with the correction function (9) (see Fig. 6).

Table I collects the results of the CASΠDFT calculations with CAS(3,3) for four different bond distances $R(N-N)$ of the triple-bonded N_2 molecule, which offers a more stringent test. Besides E_c^d, the nondynamic component E_c^{nd}, and its sum E_c, Table I displays the total E^{CAS} and E^{HF} energies in (3). Also, the standard uncorrected LYP correlation energy E_c^{LYP} is shown.

Note that DFT calculations of the correlation energy encounter the problem of the proper *ab initio* reference. The point is that conventional DFT functionals are designed to account for the total correlation, including full dynamic correlation of core and deep valence electrons. Since the H_2 molecule considered above has only a pair of outer valence electrons, calculation of the total correlation with FCI in a large basis does not present a problem. On the other hand, a reliable evaluation along the dissociation coordinate of the total correlation energy of the N_2 molecule with its $1s$ core and $2s$-type deep valence states in a moderate basis is hardly achievable with standard techniques. Because of this, schemes of the extrapolation of the HF and FCI energies to the complete basis set (CBS) limit have been developed in the literature [24].

Table II collects the reference *ab initio* data for N_2. Its first column contains the CBS HF and FCI (applied to valence electrons) energies as well as the resultant correlation energy of valence electrons E_c^{val} evaluated in Ref. [24] for the N_2 molecule at the equilibrium N-N distance $R = 2.075$ bohr.

TABLE I. The total correlation energy E_c obtained with CASΠDFT and their nondynamic E_c^{nd} and dynamic E_c^d components (in hartree) for four N-N separations (in bohr) in the N_2 molecule.

N_2 R (bohr)	2.075	3.779	4.724	5.669
E^{HF}	−108.87876	−108.32218	−108.11775	−107.99316
E^{CAS}	−108.99725	−108.78304	−108.78047	−108.77707
E_c^{nd}	−0.11849	−0.46086	−0.66272	−0.78391
E_c^d	−0.44705	−0.32995	−0.30618	−0.30132
E_c (CASΠDFT)	−0.56554	−0.79081	−0.96890	−1.08523
E_c^{LYP}	−0.48271	−0.45888	−0.45425	−0.45179

TABLE II. The reference correlation energies (in hartree) for four N-N separations (in bohr) in the N_2 molecule.

N_2 R (bohr)	2.075	3.779	4.724	5.669
E^{HF}	-108.99383	-108.35798	-108.14928	-108.02718
$E^{FCI/MRCI}$	-109.42513	-109.04420	-109.01892	-109.01575
E_c^{val}	-0.43130	-0.68622	-0.86964	-0.98857
$E_c^{FCI/MRCI}$	-0.550	-0.805	-0.989	-1.108

To obtain the total correlation energy E_c, E_c^{val} is augmented with the core correlation energy of -0.119 hartree also evaluated in [24]. For larger R, E_c^{val} is obtained in this paper as the difference between the total energies of the multireference CI (MRCI) in occupation restricted multiple active spaces (ORMAS) [25] and HF calculated in the cc-pVTZ basis. The present ORMAS includes all excitations within the full valence space (including $2s$-type deep valence states) to the three lowest virtual orbitals as well as all singles and doubles (SD) from the full valence space to the outer space.

Remarkably, the total correlation energies E_c calculated with the present CASΠDFT are rather close to the reference E_c values for all four N-N distances considered (compare Tables I and II). Note that at the equilibrium the SDC effect is rather small, so the lowering of the absolute value $|E_c^d|$ of (4) compared to the uncorrected $|E_c^{LYP}|$ is only 0.036 hartree (see Table I). As was established in the literature [26], in DFT the major part of nondynamic correlation in molecules around equilibrium is effectively provided with the DFT exchange functional. In its turn, in CASΠDFT nondynamic correlation is calculated directly via the difference (3). Evidently, the corresponding HF energy of -108.879 hartree in Table I calculated in a small basis is considerably higher than its CBS limit of -108.994 hartree in Table II. However, this basis set error is effectively compensated with that in E^{CAS}. Due to this, the resultant CASΠDFT sum (2) of -0.565 hartree is only by 0.015 hartree off its CBS limit value of -0.550 hartree (compare Tables I and II).

At larger R, LYP itself does not show the SDC effect, so E_c^{LYP} stays nearly constant at ca. -0.455 hartree (see Table I). Altogether, DFT exchange-correlation functionals fail to reproduce the build-up of strong nondynamic correlation with R. This causes the well-known problems of conventional DFT with the description of molecular dissociation, with too high energies of the spin-restricted DFT for stretched closed-shell molecules.

Then, the proposed CASΠDFT gives for N_2 the same qualitative picture of the interplay between dynamic and nondynamic correlation as for H_2, adapted to dissociation of not single, but three bonds of N_2. Again, at the equilibrium dynamic correlation (this time including the core and deep valence contributions) prevails (see Table I). At larger R, $|E_c^{nd}|$ greatly increases, due to the gradual build-up of strong nondynamic correlation in three dissociating N_2 bonds.

The accompanying SDC effect substantially decreases $|E_c^d|$ from 0.447 hartree at $R = 2.075$ bohr to 0.301 hartree at $R = 5.669$ bohr (see Table I). Apparently, this decrease is caused with the vanishing dynamic correlation of electrons of three dissociating bonds, while that of the core and deep valence electrons is expected not to alter appreciably. Yet (due to strong nondynamic correlation), the total CASΠDFT correlation energy $|E_c|$ experiences an almost twofold rise with R, which rather closely reproduces that of the reference $|E_c|$ (compare Tables I and II).

V. GROUND-STATE CORRELATION ENERGY OF THE CARBON DIMER WITH CASΠDFT

While strong nondynamic correlation characterizes the stretched H_2 and N_2, in the ground state of C_2 it takes place already for the equilibrium $R = 2.348$ bohr. Besides, the CBS data for the equilibrium C_2 was reported in Ref. [24]. This makes C_2 at the equilibrium an instructive test for the proposed CASΠDFT.

Unlike H_2 with its single paradigmatic two-electron bond and N_2 with its three bonds, the bonding in C_2 can be described as intermediate between two and four bonds. Indeed, in the C_2 wave function obtained with the full-valence space multiconfigurational self-consistent field method (MCSCF) the leading valence configuration $2\sigma^2 2\sigma^{*2} 2\pi_x^2 2\pi_y^2$ represents two π bonds [24]. However, it has a strong admixture of the configuration $2\sigma^2 3\sigma^2 2\pi_x^2 2\pi_y^2$, which formally represents four bonds. It is a combination of these two configurations including the localized $2\sigma^*$ and relatively diffuse 3σ MOs, respectively, which is responsible for strong nondynamic correlation in C_2.

This peculiar bonding pattern presents the problems for its reliable theoretical description. In particular, the strong zeroth-order multiconfigurational character of the C_2 electronic structure makes problematic its description with the conventional coupled-cluster (CC) methods. In DFT it requires the construction of the ground-state ensemble for the Kohn-Sham (KS) noninteracting system [27], in spite of the above mentioned pure-state representation of the interacting C_2 system.

In the present CASΠDFT, the CAS(3,3) with six electrons in the active space $2\sigma^* 3\sigma 2\pi_x 2\pi_y 2\pi_x^* 2\pi_y^*$ of six MOs is chosen to describe nondynamic correlation in C_2 at the equilibrium. The CASΠDFT calculations are performed in the same small cc-pVDZ basis without d functions as was employed in the previous sections for N_2. Table III displays the CASΠDFT nondynamic correlation energy E_c^{nd} together with the generic

TABLE III. Comparison of the CASΠDFT and the reference CBS correlation energies (in hartree) for the C_2 molecule at the equilibrium.

C_2, $R = 2.348$ bohr	E^{HF}	E^{CAS}	E_c^{nd}	E_c^d	E_c (CASΠDFT)	E_c^{LYP}
	-75.35713	-75.56911	-0.21198	-0.31357	-0.52555	-0.38216
	E^{HF}	E^{FCI}	E_c^{val}	E_c^{core}	E_c^{FCI}	
CBS	-75.40759	-75.81445	-0.40686	-0.1124	-0.5193	

TABLE IV. Comparison of the CASΠDFT E_c^d and reference correlation energies E_c^{FCI} (in hartree) for four H-H separations (in bohr) in the first excited $^1\Sigma_u^+$ state of the H_2 molecule.

H_2 R (bohr)	2	3	3.5	4
E^{CAS}	−0.68577	−0.70566	−0.69411	−0.67954
E^{CIS}	−0.71266	−0.70914	−0.69852	−0.68616
E^{FCI}	−0.75173	−0.75212	−0.74449	−0.73507
E_c^{CIS}	−0.02689	−0.00348	−0.00441	−0.00662
E_c^{gd}	−0.03907	−0.04298	−0.04597	−0.04891
E_c^{FCI}	−0.06596	−0.04646	−0.05038	−0.05553
E_c^d	−0.06315	−0.05544	−0.05505	−0.05413
E_c^{LYP}	−0.03205	−0.03072	−0.03001	−0.02931

E^{HF} and E^{CAS} total energies. It also compares E_c^d of (4) with the uncorrected E_c^{LYP}. Besides, Table III shows the reference data of Ref. [24]. It includes the CBS limits E^{HF} and E^{FCI} of the total HF and FCI energies (the latter includes only valence correlation), the corresponding correlation energy of valence electrons E_c^{val}, and the CBS limit E_c^{core} of the core correlation energy.

The relative strength of nondynamic correlation in C_2 can be assessed by comparing the CAS(3,3) E_c^{nd} values for C_2 and N_2. For C_2 $|E_c^{nd}|$ is nearly twice as large than that for the equilibrium N_2 (compare Tables I and III). The relative strength of nondynamic correlation also can be assessed by its SDC effect (the latter can be evaluated from the SDC correction) by taking the difference between the CASΠDFT E_c^d and E_c^{LYP}. For C_2 this difference of 0.06859 hartree (see Table III) is more than twice as large as that of 0.03092 hartree for N_2 (see Table I). This data confirms that, indeed, in C_2 nondynamic correlation is considerably stronger compared to the equilibrium N_2.

Remarkably, the total CASΠDFT correlation energy E_c, the sum of E_c^{nd} and E_c^d, reproduces closely the reference CBS limit value, the sum of E_c^{val} and E_c^{core}. The corresponding deviation is only 0.006 hartree (see Table III). Thus, also in the case of the peculiar complicated bonding pattern in C_2 the proposed CASΠDFT produces a good quality correlation energy in a small basis.

VI. EXCITED-STATE CORRELATION ENERGY ALONG THE BOND-DISSOCIATION COORDINATE WITH CASΠDFT

Table IV displays the results of the correlation energy calculations for four different bond distances R of the excited $1^1\Sigma_u^+$ state of H_2. The reference correlation energies E_c^{FCI} is calculated in the large aug-cc-pVQZ basis as the difference between the total FCI E^{FCI} and the energy E^{CAS} of the correlationless excited state Ψ_u^{CAS} mentioned in Sec. II, which are also shown in Table IV. As was already mentioned in Sec. II, in this case the only CAS configuration of the proper symmetry is just the excited HF configuration, so E_c^{nd} of (3) vanishes and E_c solely represents the effect of dynamic correlation.

First of all, note a general enhancement of dynamic correlation represented by E_c compared to the ground state. Indeed,

at all R the absolute E_c of Table IV are much larger, than the largest ground-state equilibrium $|E_c^d| = 0.02809$ hartree displayed in Fig. 6, and they are even larger than the total equilibrium FCI energy $|E_c| = 0.04045$ hartree, which also contains the contribution of nondynamic correlation. This can be anticipated from the qualitative arguments of Sec. II on the relative magnitude of $x((r))$ for the ground and excited states.

On top of this general enhancement background, one can notice the nonmonotonic dependence of E_c on R. Specifically, $|E_c|$ is the largest for the shortest $R = 2$ bohr, it reaches the minimum at $R = 3$ bohr, and it continues its rise for larger R (see Table IV). In order to rationalize this complicated behavior, E_c is partitioned as follows:

$$E_c = E_c^{CIS} + E_c^{gd}. \tag{13}$$

Here, the first term is the correlation contribution from CI with single (CIS) excitations from the CAS reference,

$$E_c^{CIS} = E^{CIS} - E^{CAS}, \tag{14}$$

while the remainder E_c^{gd} associated in the considered case of H_2 with double excitations can be called the energy of "genuine" dynamic correlation.

One can see from Table IV, that $|E_c^{gd}|$ monotonically increases with R. This, together with the increase of $x(r)$ with R shown in Sec. II, indicates the enhancement of genuine dynamic correlation with the increase of the ionic character of the excited state. It is E_c^{CIS}, which is responsible for the nonmonotonic behavior of the total E_c. The absolute value of E_c^{CIS} drops from 0.027 hartree at $R = 2$ bohr to only 0.003 hartree at $R = 3$ bohr and then increases somewhat to 0.007 hartree at $R = 4$ bohr. With this, the CIS correlation counters the increase of the CAS energy, when going from its minimal value at $R = 3$ bohr. This countereffect of CIS is the largest for the "squeezed" excited state at $R = 2$ bohr.

The above mentioned nonmonotonic pattern of correlation in the excited state is to be reproduced with a nonmonotonic dependence of the EDC segment (11) on $x(r)$. This is so, since, as was shown in Sec. II, the structure with the enhanced CIS correlation effect at $R = 2$ bohr is characterized with smaller $x(r)$, than those of the structure with $R = 4$ bohr (compare Figs. 4 and 5). To accomplish this, $P^{EDC}(x(r))$ of (11) consists of two terms. The first term with $c = 2.6$ provides the above mentioned general EDC in the excited state, while its second term with $g = 1.5$ introduces the required nonmonotonic dependence on $x(r)$.

One can see from Table IV, that the total correction function (9) enhances the electron correlation compared to the LYP functional, so that the absolute E_c^d values are substantially larger than the E_c^{LYP} ones. This means that the enhancement segment $P^{EDC}(x(r)) > 1$ for $x(r) > 1$ brings the dominant contribution in this case.

This enhancement moves E_c^d values rather close to the reference E_c ones. CASΠDFT qualitatively reproduces the decrease of $|E_c|$ with the decreasing CIS correlation, when going from $R = 2$ to $R = 3$ bohr. Admittedly, it replaces the increase of $|E_c|$ beyond $R = 3$ bohr with a near saturation of E_c^d. Nevertheless, at the shortest separation $R = 2$ bohr the deviation between E_c^d and E_c is only 0.003 hartree, while at the longest separation $R = 4$ bohr CASΠDFT correlation

energy error reaches its minimum of just ca. 0.001 hartree (see Table IV).

VII. CONCLUSIONS

In this paper it is shown that the on-top pair density, in the form of its ratio $x(\boldsymbol{r})$ to the uncorrelated counterpart, can meaningfully describe both the local effect of nondynamic correlation and that of excitation to a state of the ionic nature on the electron distribution. The opposite trends in dynamic correlation caused by these effects, SDC by (strong) nondynamic correlation and EDC by excitation, are elucidated by considering the corresponding changes of the conditional density.

Based on this description in terms of the "effective" densities, the correction function to the conventional DFT correlation functionals is proposed. It accounts for both SDC and EDC, so it is physically meaningfully defined in the whole range of the $x(\boldsymbol{r})$ variation. One can consider it as a step forward compared to the previous work [15], in which for the correction function to the whole exchange-correlation functional the argument $x(\boldsymbol{r})$ was cut off at $x = 1$ for $x > 1$. Then, the correction function of this paper describes in the region $x > 1$ the nonmonotonic dependence of the correction on $x(\boldsymbol{r})$ caused by the interplay of the correlation contributions from CIS and "genuine" dynamic correlation.

The CASΠDFT scheme of the calculation of the total correlation energy is proposed. In this scheme, nondynamic correlation is taken into account with the CAS(n,n), while dynamic correlation is evaluated with the LYP functional corrected with the developed correction function. This proposed CASΠDFT reproduces rather closely the reference data on single-bond stretching in H_2 and on triple-bond stretching in N_2. Based on the present result, we can conclude that it is the neglect of SDC, which is responsible for double counting of electron correlation in the ground state, when an uncorrected DFT correlation functional is combined with CAS(n,n). Furthermore, CASΠDFT closely reproduces the reference correlation energy for the C_2 molecule, a peculiar system where strong nondynamic correlation surfaces already at the equilibrium.

The proposed CASΠDFT offers a promising scheme of evaluation of the total correlation energy in a small basis, since it requires only rather inexpensive CAS(n,n) and ΠDFT in such a basis. Thus, it exploits the relative insensitivity of DFT calculations to the basis choice. Furthermore, the present results demonstrate the ability of CAS(n,n) to produce an adequate description of nondynamic correlation in a small basis.

The present results illustrate the well-known problem of conventional DFT with the description of molecular bond breaking. In particular, the standard LYP functional yields almost constant correlation energies along the bond-dissociation coordinate. Nevertheless, with the additional information provided with the CAS on-top pair density, it can serve as the basis of the corrected description of the electron correlation with the proper account of both SDC and EDC.

[1] N. C. Handy and A. J. Cohen, Mol. Phys. **99**, 403 (2001).

[2] B. O. Roos, in *Advances in Chemical Physics: Ab Initio Methods in Quantum Chemistry*, Part 2, edited by K. P. Lawley (John Wiley & Sons, Hoboken, NJ, 1987), Vol. 69, pp. 399–445.

[3] K. Andersson, P.-A. Malmqvist, B. O. Roos, A. J. Sadlej, and K. Wolinski, J. Phys. Chem. **94**, 5483 (1990).

[4] J. Olsen, J. Quantum Chem. **111**, 3267 (2011).

[5] K. Raghavachari and J. B. Anderson, J. Phys. Chem. **100**, 12960 (1996).

[6] S. H. Vosko, L. Wilk, and M. Nusair, Can. J. Phys. **58**, 1200 (1980).

[7] C. Lee, W. Yang, and R. G. Parr, Phys. Rev. B **37**, 785 (1988).

[8] J. P. Perdew, J. A. Chevary, S. H. Vosko, K. A. Jackson, M. R. Pederson, D. J. Singh, and C. Fiolhais, Phys. Rev. B **46**, 6671 (1992).

[9] J. P. Perdew, K. Burke, and M. Ernzerhof, Phys. Rev. Lett. **77**, 3865 (1996).

[10] A. D. Becke, A. Savin, and H. Stoll, Theor. Chim. Acta **91**, 147 (1995).

[11] B. Mielich, H. Stoll, and A. Savin, Mol. Phys. **91**, 527 (1997).

[12] J. J. W. McDouall, Mol. Phys. **101**, 361 (2003).

[13] S. Gusarov, P.-A. Malmqvist, and R. Lindh, Mol. Phys. **102**, 2207 (2004).

[14] E. Hedegard, S. Knecht, J. S. Kielberg, H. J. Jensen, and M. Reiher, J. Chem. Phys. **142**, 224108 (2015).

[15] G. Li Manni, R. K. Carlson, S. Luo, D. Ma, J. Olsen, D. G. Truhlar, and L. Gagliardi, J. Chem. Theory Comput. **10**, 3669 (2014).

[16] E. Fromager, J. Toulouse, and H. J. Jensen, J. Chem. Phys. **126**, 074111 (2007).

[17] B. Miehlich, A. Savin, H. Stoll, and H. Preuss, Chem. Phys. Lett. **157**, 200 (1989).

[18] M. Gaus, Q. Cui, and M. Elstner, J. Chem. Theory Comput. **7**, 931 (2011).

[19] J. T. H. Dunning, J. Chem. Phys. **53**, 2823 (1970).

[20] J. T. H. Dunning, J. Chem. Phys. **90**, 1007 (1989).

[21] M. W. Schmidt, K. K. Baldridge, J. Boatz, S. Elbert, M. Gordon, J. Jensen, S. Kosekt, N. Matsunaga, K. Nguyen, S. Su *et al.*, J. Comput. Chem. **14**, 1347 (1993).

[22] M. S. Gordon and M. W. Schmidt, in *Theory and Applications of Computational Chemistry: The First Forty Years*, edited by C. E. Dykstra, G. Frenking, K. S. Kim, and G. E. Scuseria (Elsevier, Amsterdam, 2005), pp. 1167–1189.

[23] R. K. Carlson, D. G. Truhlar, and L. Gagliardi, J. Phys. Chem. A **121**, 5540 (2017).

[24] L. Bytautas and K. Ruedenberg, J. Chem. Phys. **122**, 154110 (2005).

[25] J. Ivanic, J. Chem. Phys. **119**, 9364 (2003).

[26] P. R. T. Schipper, O. V. Gritsenko, and E. J. Baerends, Phys. Rev. A **57**, 1729 (1998).

[27] P. R. T. Schipper, O. V. Gritsenko, and E. J. Baerends, Theor. Chem. Acc. **99**, 329 (1998).